# Comparison of Real-Time Methods for Maximizing Power Output in Microbial Fuel Cells

**L. Woodward, M. Perrier, and B. Srinivasan**
École Polytechnique de Montréal, Dept. of Chemical Engineering, Montreal, Canada, H3C 3A7

**R. P. Pinto and B. Tartakovsky**
École Polytechnique de Montréal, Dept. of Chemical Engineering, Canada, H3C 3A7, and Biotechnology Research Institute, National Research Council, Montreal, Canada, H4P 2R2

*DOI 10.1002/aic.12157*
*Published online March 29, 2010 in Wiley Online Library (wileyonlinelibrary.com).*

*Microbial fuel cells (MFCs) constitute a novel power generation technology that converts organic waste to electrical energy using microbially catalyzed electrochemical reactions. Since the power output of MFCs changes considerably with varying operating conditions, the online optimization of electrical load (i.e., external resistance) is extremely important for maintaining a stable MFC performance. The application of several real-time optimization methods is presented, such as the perturbation and observation method, the gradient method, and the recently proposed multiunit method, for maximizing power output of MFCs by varying the external resistance. Experiments were carried out in two similar MFCs fed with acetate. Variations in substrate concentration and temperature were introduced to study the performance of each optimization method in the face of disturbances unknown to the algorithms. Experimental results were used to discuss advantages and limitations of each optimization method.* © 2010 American Institute of Chemical Engineers *AIChE J,* 56: 2742–2750, 2010
*Keywords: maximum power point tracking, real-time optimization, perturbation and observation method, microbial fuel cell, multiunit optimization*

## Introduction

Resource availability and environmental concerns have increased the urgency to search for renewable energy sources. Besides photovoltaic and wind energy systems, fuel cell technology is emerging as a viable option. However, the main drawback of traditional hydrogen based fuel cells is the need for the generation of hydrogen and its transportation to the point of use. On the other hand, microbial fuel cells (MFCs) can be used to generate electrical energy from a variety of carbon sources, including wastewater with varying concentrations of organic matter.

In a MFC, anodophilic microorganisms degrade organic matter and transfer electrons to the anode.[1–3] Since the late 90s, when intensive MFC research began, power density in MFCs has increased by several orders of magnitude.[4] Yet, the attainable power density of a single MFC is low and the working voltage is limited to 0.3–0.5 V. Consequently, active research is on-going to increase the electrical power delivered by MFCs. This research involves improved reactor

Correspondence concerning this article should be addressed to B. Tartakovsky at boris.tartakovsky@nrc-cnrc.gc.ca.

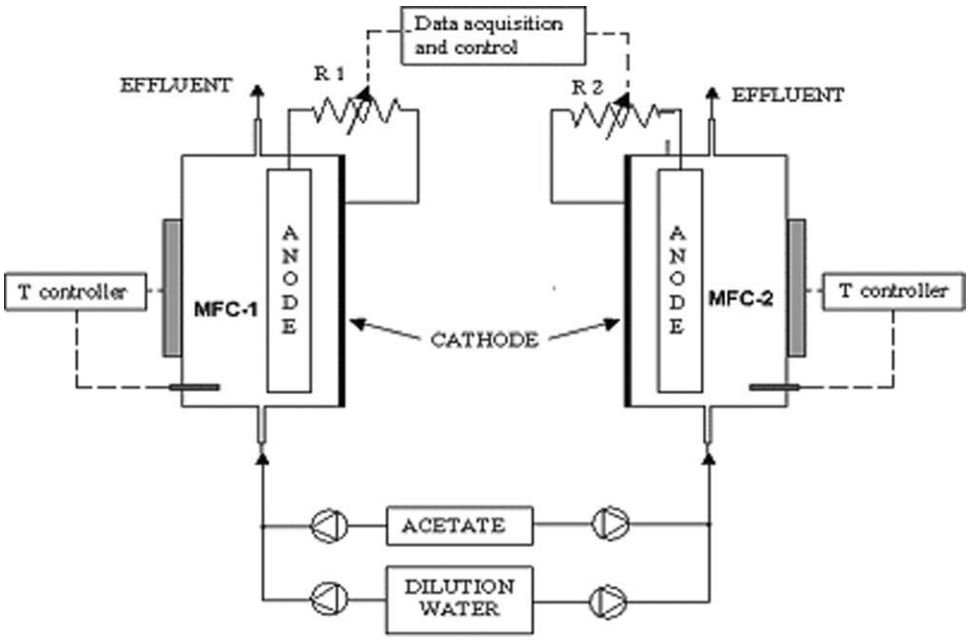


**Figure 1. Experimental setup showing two simultaneously operated MFCs.**

design such as an air cathode,[5] tubular,[6,7] and upflow MFCs,[8,9] improved electrode design,[10,11] and improved system design where a stack of MFCs is used to increase output voltage and/or power.[12–14]

One of the simplest ways of increasing the power output of an electric power source is to always maintain an electrical load that corresponds to the maximum power output. As a higher current is drawn the voltage drops and the maximum power output is obtained when the external resistance equals the internal resistance of the power source. More than 50% of the power can be lost if the electrical load is not matched with the internal resistance. This problem has been addressed for several types of electric power sources such as photovoltaic (PV) systems[15] and hydrogen fuel cells[16] by online optimization of the electrical load. Often a DC/DC converter and a buffer are inserted between the PV array, and the electrical load and the duty cycle ratio or the current drawn by the DC/DC converter is optimized using a maximum power point tracking (MPPT) method.[16,17]

Several MPPT methods for photovoltaic systems have been reported in the literature. One class of MPPT methods uses a mathematical model of the solar panel to compute the impedance.[18] The main drawback of such an approach is that the model is too complex and a lot of parameters can vary. In the context of MFCs, this approach is difficult to implement because of the complexity, the nonlinearity and the nonstationarity of microbial kinetics.[19,20] Another class of methods does not use a fundamental model for optimization purposes. Perturbation and observation (P/O) and gradient methods are nonmodel based real-time optimization methods used as MPPT in photovoltaic systems.[21] These methods consider the system dynamics to be fast, which is justified for photovoltaic systems where the time of convergence to the optimum is in the order of seconds. P/O method is widely used due to its simplicity and robustness, while fast convergence was reported for the gradient method.[22]

Power output of a MFC depends on many operational parameters like carbon source (fuel) composition and concentration, temperature, and pH.[23,24] Furthermore, voltage reversal was observed in a stack of MFCs operated at a nonoptimal electrical load.[13] Large variations in wastewater concentration and flow rate make the optimization of electrical load a prerequisite for practical MFC applications.

The main difference between photovoltaic systems and MFCs is that the latter exhibit a time-dependent response with relatively slow dynamics with characteristic times in the order of minutes to dozens of minutes, which might affect performance of MPPT methods. This study presents a comparison of the P/O method, the gradient method and the recently developed multiunit (MU) optimization method[25,26] for optimizing external resistance of a MFC.

## Materials and Methods

Experiments were carried out in two continuous flow air-cathode membraneless MFCs. A schematic diagram of the experimental setup is shown in Figure 1. Each MFC was constructed with a series of polycarbonate plates.[27] The anodic chamber volume of each cell was 50 mL. The anode was made of a 5 mm thick graphite felt measuring 10 $\times$ 5 cm (GFA5, Speer Canada, Kitchener, ON, Canada). The cathode was made of a 10 $\times$ 5 cm gas diffusion electrode with a Pt load of 0.5 mg $cm^{-2}$ (GDE LT 120EW, E-TEK Division, PEMEAS Fuel Cell Technologies, Somerset, NJ, USA). The distance between the anode and cathode was 0.5 cm.

The MFCs were inoculated with 5 mL of homogenized anaerobic sludge (Lassonde Industries, Inc., Rougemont, QC, Canada) and operated at the same temperature and organic load. A stock solution of carbon source containing 40 g $L^{-1}$ of acetate was fed using an infusion pump (model PHD 2000, Harvard Apparatus, Canada) at a rate of 0.1–0.2 mL

$h^{-1}$. One mL of trace metals stock solution was added to 1 L of the dilution water. The stock solutions of acetate and trace metals were prepared according to Tartakovsky et al.[27] All solutions were sterilized and maintained at 4°C until use.

The dilution water was fed to each MFC at a rate of 6.08 mL $h^{-1}$ using peristaltic pumps (Cole-Parmer, Chicago, IL, USA), and providing a retention time of 10 h. Peristaltic pumps also were used for liquid recirculation at a rate of 0.57 L $h^{-1}$ in the external recirculation loop. Heating plates (5 × 10 cm) located on the anodic chamber sides of the MFCs and thermocouples placed in the anodic chamber and connected to temperature controllers (Model JCR-33A, Shinko Technos Co., Ltd. Osaka, Japan) maintained preset temperatures. For each MFC, a computer controlled digital potentiometer with a data acquisition board (Innoray, Montreal, QC, Canada) provided a resistor variation range from 8 to 252 Ω.

Acetate concentration was determined using a gas chromatograph (Sigma 2000, Perkin-Elmer, Norwalk, Connecticut, USA) equipped with a 91 cm × 4 mm i.d. glass column packed with 60/80 Carbopack C/0.3% Carbopack 20 NH3PO4 (Supelco, Mississauga, Ontario, Canada). More details on analytical methods and media composition are provided in Tartakovsky et al.[27]

Polarization curves (voltage vs current) were acquired by periodically changing MFC external resistance, measuring the resulting voltage and calculating current ($I$, in mA) as $I = V/R$, where $V$ is the voltage (mV), and $R$ is the external resistance. A time interval of 10 min was allowed before each measurement. Power output ($P$, mW) was calculated as $P = I{\cdot}V$. MFC performance was visualized by plotting the resulting power output vs. current (power curve) or vs. external resistance. Slope of the linear part of the polarization curve was used to estimate the internal resistance of MFCs.

## Problem Definition and Method Description

### *Optimization problem*

The problem addressed in this article is the maximization of power output of a MFC by adjusting external resistance. The optimization problem can be formulated as follows

$$\max_R P = \max_R \frac{V^2}{R} \tag{1}$$

where $P$ is the power delivered by the microbial fuel cell through the external variable resistance $R$ and $V$ is the measurable MFC voltage. A real-time optimization method will be used to adjust the value of the external resistance in order to maximize the electrical power delivered through the external resistances at each moment.

The problem definition presented previously is slightly different from that commonly used in PV systems, where a DC/DC converter and a buffer are used to control the electrical load. In this case, the manipulated variable of the optimization method is the duty cycle ratio or the current drawn by the DC/DC converter.[17] Here, external resistance ($R$) is chosen as the manipulated variable to simplify the experimental procedure.

## Maximum Power Point Tracking Methods

### *Perturbation and observation method*

The P/O method is commonly used in MPPT.[28] Herein, the amplitude of each resistance change is fixed and is equal to a predetermined offset $\Delta R$. The direction of resistance change depends on the sign of gradient, which is determined using the finite difference method, that is, by comparing the value of the objective function (after the resistance change) with that at the previous resistance. Due to the influence of process dynamics, it is important to attain a pseudo steady state after each resistance change. The method can be expressed as follows

$$R(k+2) = R(k+1) + \Delta R \,\mathrm{sign}\left(\frac{P(k+1) - P(k)}{R(k+1) - R(k)}\right) \tag{2}$$

where $\Delta R$ is the perturbation on the input $R$, $P$ is the power output, and $k$ is iteration number. As $k \to \infty$, due to the presence of a fixed perturbation $\Delta R$, the resistance values will oscillate around an average point $R_{eq}$, with amplitude of $\Delta R$

$$R(k) = \begin{cases} R_{eq} + \Delta R \\ \text{or} \\ R_{eq} - \Delta R \end{cases} \tag{3}$$

Also, since $\Delta R$ is the minimum step that is taken, the maximum distance between the average of the oscillation ($R_{eq}$), and the true optimum ($R^*$) is $\Delta R/2$

$$R_{eq} - R^* \le \frac{\Delta R}{2} \tag{4}$$

A higher $\Delta R$ can be used to increase the speed of convergence, but will result in a larger error in estimating optimal external resistance and in more oscillations. Thus, a compromise between the convergence rate and the method accuracy might be required.

### *Gradient method*

The Gradient method[29] also uses a constant perturbation $\Delta R$ to estimate the gradient. The main difference from the P/O method is that the amplitude of the move is proportional to the value of the estimated gradient

$$\begin{aligned} R(k+1) &= R(k) + \Delta R \\ R(k+2) &= R(k) + \alpha_{grad}\left(\frac{P(k+1) - P(k)}{R(k+1) - R(k)}\right) \end{aligned} \tag{5}$$

where $\alpha_{grad}$ is an appropriately chosen gain. Note that every iteration of this method has two steps: (1) a constant amplitude step to evaluate the gradient, and (2) a variable amplitude step based on the value of the gradient. Assuming that the method is well tuned, and at $k \to \infty$ it converges to the true optimum $R^*$, the $R$ values will oscillate between the point resulting from the constant perturbation at an amplitude $\Delta R$, and the other point resulting from the optimization step, which depends on the gradient value. At $k \to \infty$ these two points should be placed at each side of the oscillation average $R_{eq}$, where $R_{eq} =$

$R^*$, with a distance of $\Delta R$ between them. Thus, the first point is placed at $R_{eq}-\Delta R/2$, and the second point at $R_{eq}+\Delta R/2$ with no additional error, that is, $R_{eq}=R^*$, as opposed to what was discussed for the P/O method. The maximum amplitude of oscillation is also halved.

The convergence rate of this method can be improved by choosing a higher value for the gain. However, too high a gain could lead to a behavior where the system does not converge to an equilibrium point, thus, the main difficulty lies in the proper choice of this parameter. Also, the value of the gain depends very much on the second derivative (curvature) of the power curve, which could change in time.

### *Multiunit optimization method*

The multiunit (MU) optimization method assumes the presence of two identical MFCs.[25] These two units are operated with an offset $\Delta R$ between them. The gradient is estimated by finite differences between the values of the objective function obtained for each MFC. The two units follow the same control law and always keep the $\Delta R$ difference from each other.

In practice, the units are similar but not perfectly identical, and the multiunit optimization method can force the system to converge far away from the optimum. If the differences in the static characteristics $\beta$ and $\gamma$ are defined as in Figure 2A, correctors can be inserted into the multiunit loop in order to compensate for the differences in the static characteristics[26] as shown in Figure 2B, where $\hat{\beta}$ and $\hat{\gamma}$ are the correctors introduced.

In this work, since the difference between the optimal resistances of the MFCs do not vary significantly, $\hat{\beta}$ is kept at a constant preset value and $\hat{\gamma}$ is re-evaluated online by periodically removing the offset of $\Delta R$ between the units. Thus, two intervals are present: the optimization interval, where the adaptation law given in the following Eqs. 6–8 is used, and the parameter estimation interval, where the adaptation law given in Eqs. 9–11 is used

$$\hat{g}(k) = \left(\frac{P_2(k)-P_1(k)}{R_2(k)-R_1(k)}\right) = \left(\frac{P_2(k)-\hat{\gamma}-P_1(k)}{\Delta R}\right) \quad (6)$$

$$R_1(k+1) = R_1(k) + \alpha_{mu}(\hat{g}(k)) \quad (7)$$

$$R_2(k+1) = R_1(k+1) + \Delta R - \hat{\beta} \quad (8)$$

$$\hat{\gamma}(k+1) = (P_2(k) - P_1(k)) \quad (9)$$

$$R_1(k+1) = R_1(k) \quad (10)$$

$$R_2(k+1) = R_1(k+1) - \hat{\beta} \quad (11)$$

where $\alpha_{mu}$ is the MU method gain.

Since the perturbation $\Delta R$ is not time-dependent, the slow dynamics of the MFC will not affect the gradient estimation. The influence of MFC dynamics is eliminated by calculating the finite differences while estimating the gradient. Thus, the adaptation could be relatively fast. However, the time used for the $\hat{\gamma}$ corrector has to be chosen in accordance with the response time of the MFC. During the correction period, the MFCs exhibit different dynamics, and it is important to wait until the transient period is finished and the systems reach a new steady-state.

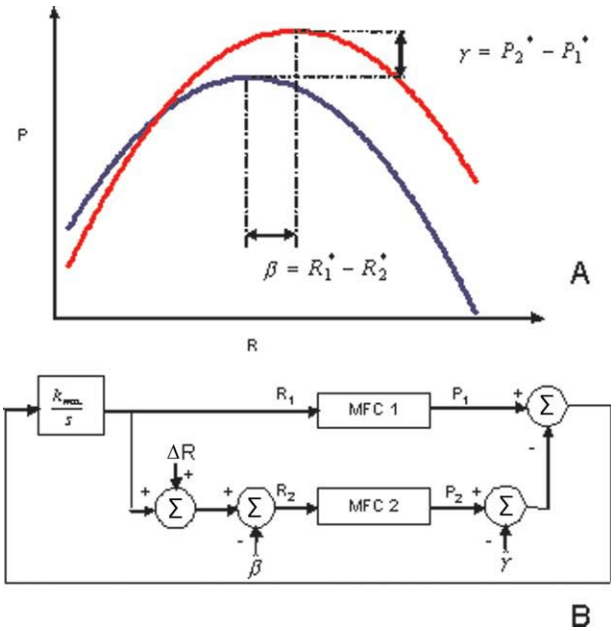


**Figure 2. (A) An example of two MFCs with different static characteristics, and (B) diagram of a multiunit optimization loop with correctors.**

[Color figure can be viewed in the online issue, which is available at wileyonlinelibrary.com.]

Applying the MU method to a process with identical units (i.e., without any correctors) brings the two units to converge to a distance of $\Delta R/2$ from the optimum without any oscillations around these points. If the two units are not perfectly identical, the adaptation of $\hat{\gamma}$ corrector requires that the two units are periodically operated at the same operating point for $\hat{\gamma}$ correction. During normal operation the MU method needs a $\Delta R$ offset between the operational points of the two units. In this work, MFC 1 is chosen as the reference unit and always remains at the same reference point ($R_1$), while MFC 2 external resistance is changed from $R_1+\Delta R-\hat{\beta}$ (for MU adaptation, see Eq. 8) to $R_1-R_1-\hat{\beta}$ (for $\hat{\gamma}$ adaptation, see Eq. 11). In the best case, when the correctors have converged to their true values, MFC 1 will converge to $R_1^*-\Delta R/2$, and MFC 2 will oscillate between $R_2^*-\Delta R/2$ and $R_2^*+\Delta R/2$, with $R_1^*$ and $R_2^*$ being the real optima of MFC 1 and MFC 2, respectively.

## Results and Discussion

### *MFC startup and characterization*

At the startup, the anodic chambers were inoculated with anaerobic sludge and acetate was fed at a rate of 200 mg $d^{-1}$. The startup external resistances for both MFCs were set at 250 Ω. A voltage increase was observed after five days of MFC operation. A period of two weeks was required to achieve a steady state, and then MFC performance was assessed by acquiring polarization and power curves. These curves were obtained for each MFC by varying the external resistances as described in the Materials and Methods section. Results are presented in Figure 3. The linear parts of

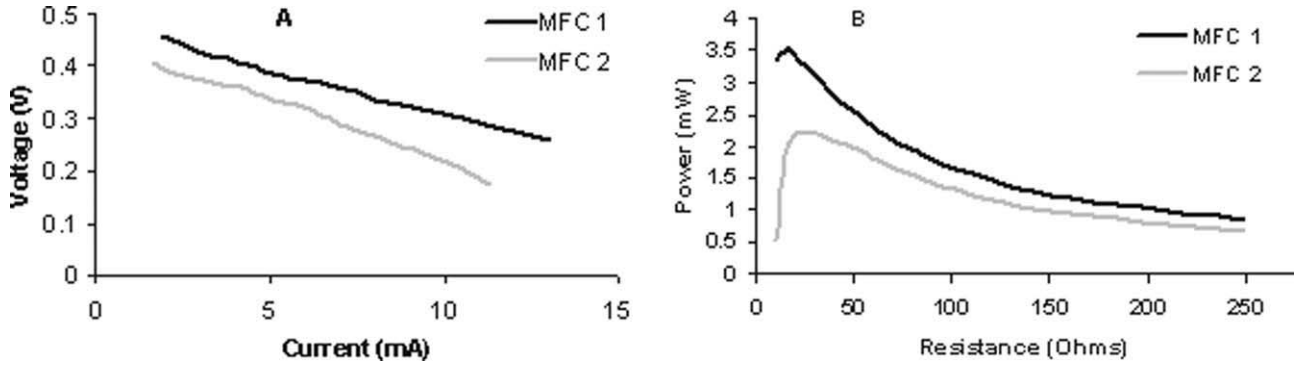


**Figure 3. Polarization (A), and power (B) curves obtained for the two MFCs.**

the polarization curves in Figure 3A represent ohmic losses. These losses are caused by ionic transport resistance in the electrolyte, the resistance of the electrode material, and contact losses.[30] Although the two MFCs were identically constructed, a comparison of the polarization and power curves in Figure 3 suggest higher ohmic losses and a mass-transfer limitation in MFC 2. Perhaps different distances between the electrodes and/or variations in biofilm thickness contributed to a higher ohmic resistance and a higher mass-transfer limitation in MFC 2. Estimation of MFC internal resistances using linear parts of the polarization curves yielded values of 15 and 23 Ω for MFC 1 and MFC 2, respectively. To optimize power output of each MFC, the MPPT method should change the external resistance of the corresponding MFC so that it is equal to the internal resistance. The difference in MFC performances highlighted the importance of optimal resistance control, as the operation of both MFCs at the same external resistance would lead to either underload of MFC 1, or poor performance of MFC 2.

Overall, polarization tests led to the following conclusions: (1) The optimal resistances and maximum power outputs of the MFCs are different ($R_1 \approx 15\ \Omega$, $R_2 \approx 23\ \Omega$, and $P_1 \approx 3.5$ mW, $P_2 \approx 2.2$ mW), and (2) the curvature of the $P$ vs. $R$ curves are not the same and are not constant for all values of $R$. In addition, "bump" tests showed that the response times are similar for both MFCs and are approximately 1 min (results not shown).

### *Optimization tests*

The P/O method described previously was tested using a time interval of 1 min between resistor changes and a perturbation $\Delta R$ of 2.5 Ω. The test was simultaneously carried out for both MFCs. Before the optimization test the two potentiometers were set to a value of 70 Ω. The results given in Figure 4A show that the maximal power is reached in about 25 min.

Tests of external resistance optimization using Gradient method were performed simultaneously for two MFCs with the same initial conditions and intervals between resistance changes as in the P/O test. The gains were adjusted by trial and error to values of 150 and 200 for MFC 1 and MFC 2, respectively. Figure 4B shows that MFC 2 converged to its optimal point of operation in 30 min, while MFC 1 failed to converge despite several attempts to tune the gain. If a

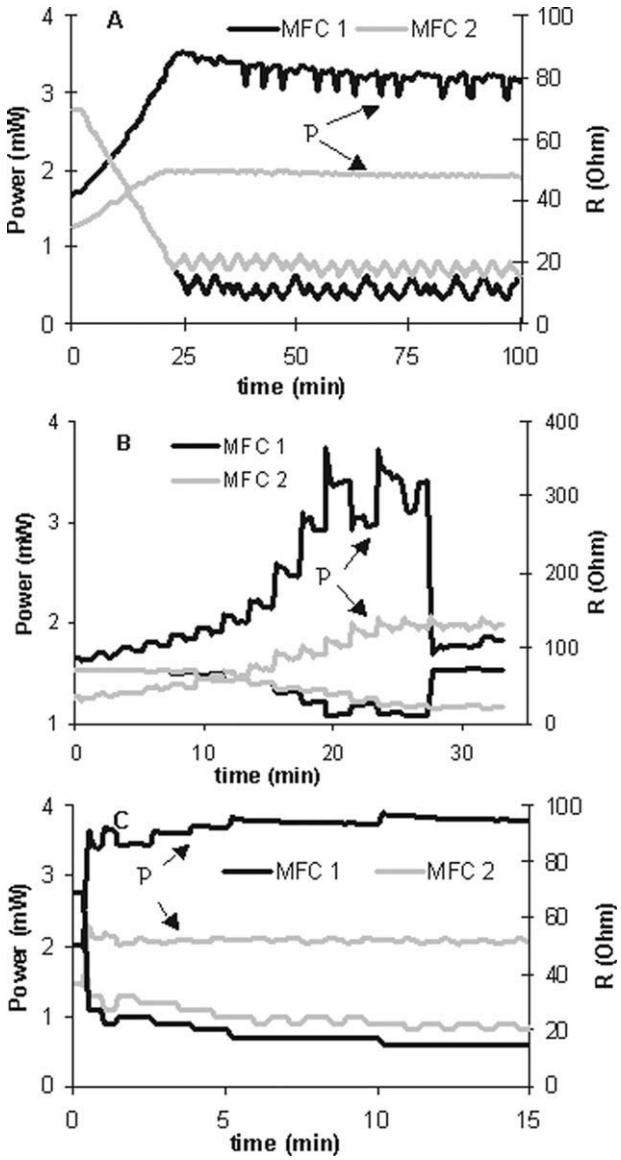


**Figure 4. Online optimization with $\Delta R$ = 2.5 Ω and a time interval between resistance changes $\Delta t$ = 1 min.**

(A) P/O method, (B) gradient method, and (C) MU method with $\Delta t = 1$ min for evaluation.

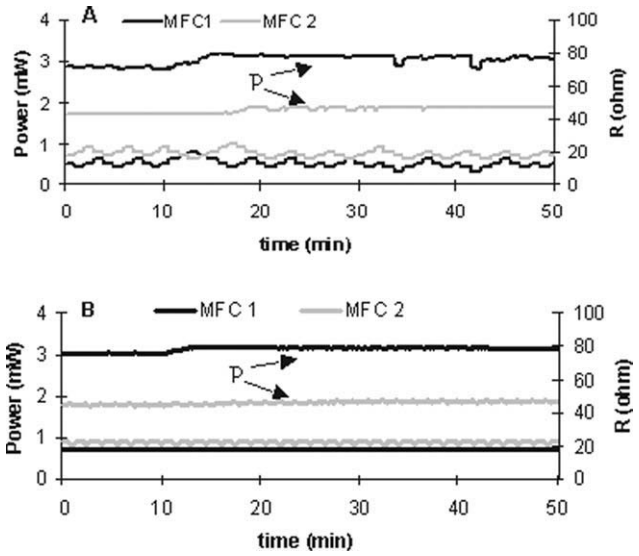


**Figure 5. Optimization methods response to acetate injection.**

(A) P/O method ($\Delta R = 2.5\ \Omega$, $\Delta t = 1$ min), (B) MU method ($\Delta R = 2.5\ \Omega$, estimation at $\Delta t = 1$ min, gain of 30 $\Omega^2$/mW).

smaller gain was used, the system stayed near the initial value, while a larger gain caused instability around the optimum. Large variations in the curvature of the polarization curve of MFC 1 resulted in a very narrow range of gains for which this method could converge.

Figure 4C shows results obtained with the MU method using a time between multiunit adaptations of 30 s, a 1 min parameter estimation period for $\hat{\gamma}$ corrector estimation, a constant $\hat{\beta} = -8\ \Omega$, an initial value of $\hat{\gamma} = -1.45$ mW, and a gain for MU adaptation $\alpha_{mu} = 40\ \Omega^2\ mW^{-1}$. The offset and the initial external resistance for these tests were the same as in the tests described earlier. With the MU method, the convergence time was considerably reduced: the multiunit scheme without adaptation converged in about 1 min to values of 22.6 Ω and 27.5 Ω for MFC 1 and MFC 2, respectively (Figure 4C). Fine tuning of the $\hat{\gamma}$ corrector to account for differences between two MFCs required another 8 min after which resistances stabilized at 15.2 Ω and 22.6 Ω (Figure 4C).

### *Tracking optimum in the presence of external perturbations*

As shown previously, the P/O and MU methods were able to correctly identify the optimal external resistances. These methods were chosen to study optimum tracking in the presence of external perturbations. The tests involved a change in substrate concentration and a change in anodic chamber temperature.

In the first test, 1 mL of the acetate stock solution containing 40 g $L^{-1}$ of acetate was injected into anodic chambers of each MFC. The response of the P/O method to substrate injection is shown in Figure 5A. The substrate concentration increased at approximately $t = 9$ min for MFC 1 and $t = 12$ min for MFC 2 (Figure 5A). Prior to acetate injection its concentration in the anodic chamber was around 200 mg $L^{-1}$. Likely, at this concentration the reaction rate were not limited by acetate availability. Consequently, the increase in observed power output was moderate in both MFCs. Variations in power output were accompanied by small variations in the external resistance values. However, since the substrate did not limit the reaction rate, the optimal resistance was unchanged, and the method returned the resistances back to their original values.

Figure 5B shows the behavior of the MU method during a similar test. Once again, acetate concentration at the test startup was 150–200 mg $L^{-1}$. It can be seen that the resistance values were not changed at all. From the perspective of the method, as power output increases in both MFCs, the difference, that is, the gradient is not affected and no resistance changes are required.

In the second perturbation test anodic chamber temperatures were changed by a temperature set point increase from 25°C to 28°C for MFC 1, and from 25°C to 31°C for MFC 2. Figure 6 shows the response of both optimization methods to this perturbation. In both MFCs the power output increased while optimal resistance decreased with increasing temperature. The observed increase in power output of MFCs agrees with Arrhenius-like dependence of microbial kinetics on temperature.[31] The external resistance decrease is less pronounced in the P/O method, partly due to oscillations and also due to the fact that an increasing power output leads to an oscillatory behavior of the method.

### *Influence of the frequency of the perturbation on the equilibrium point*

A comparison of the results showed that the time of convergence of the P/O method is longer than the one obtained with the MU optimization. This raises a question: how can

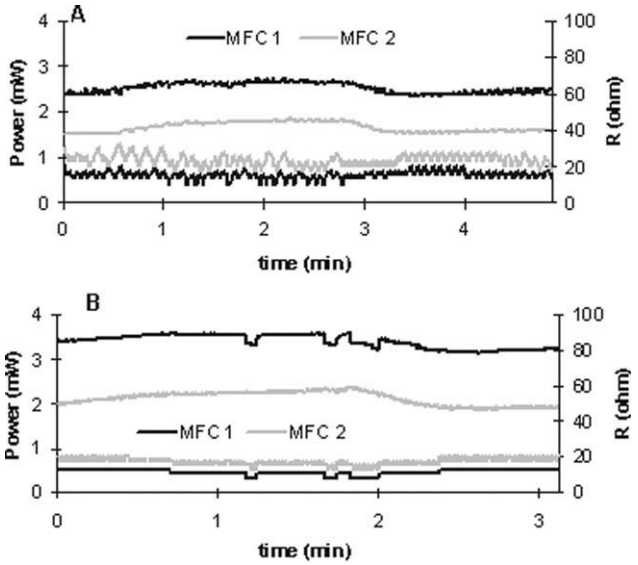


**Figure 6. Optimization methods response to temperature variation.**

(A) P/O method ($\Delta R = 2.5\ \Omega$, $\Delta t = 1$ min), and (B) MU method ($\Delta R = 2.5\ \Omega$, corrector delay $\Delta t = 1$ min, a gain of 30 $\Omega^2$/mW).

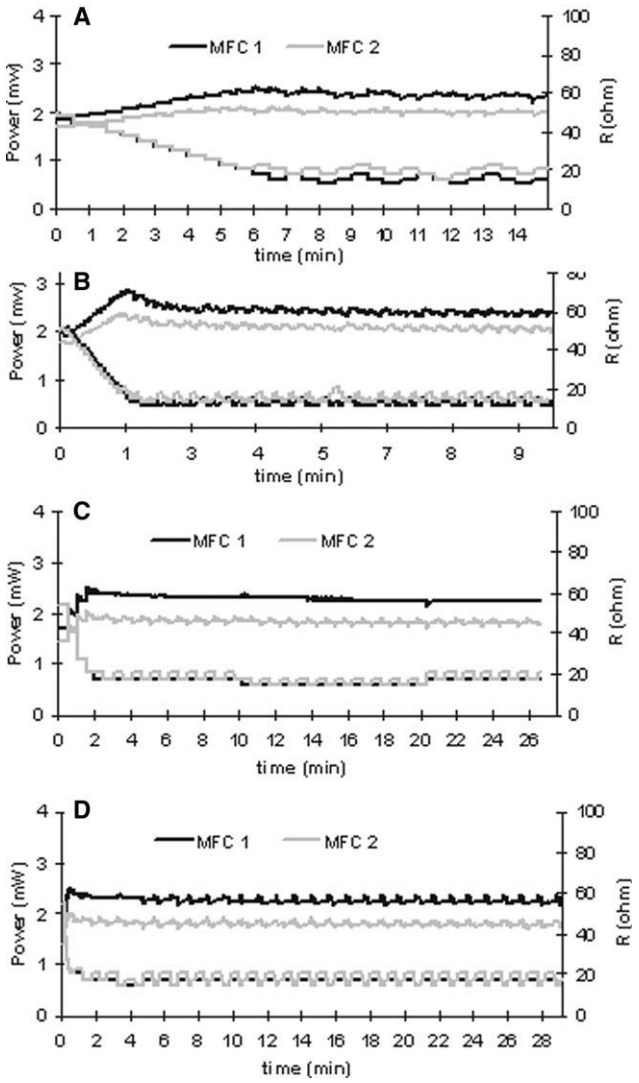


**Figure 7. Optimization using the methods with $\Delta R$ = 2.5 Ω.**

(A) P/O method with $\Delta t$ = 30 s, (B) P/O method with $\Delta t$ = 5 s, (C) MU method with time intervals of 30 s and 30 s for MU adaptation and adaptation, respectively, and (D) MU method with time intervals of 5 s and 30 s for MU adaptation and adaptation, respectively.

the time of convergence of the PO method be reduced? One way would be to increase the value of $\Delta R$ in order to make larger resistance increments. The P/O method with a $\Delta R$ of 4 Ω, instead of 2.5 Ω, reduced the time of convergence from 25 min to 12.5 min (results not shown). However, this reduction in time of convergence comes with an increase in oscillations around the optimum. The choice of $\Delta R$ is then a compromise between the rate of convergence and the accuracy of the optimal value of power reached.

Another way to reduce the time of convergence of the P/O method is to reduce the delay between the perturbations, that is, to increase the frequency of the perturbation. Figure 7A and B shows application of the P/O method at a $\Delta R$ of 2.5 Ω, and delays between each resistance change of 30 s and 5 s, respectively. The results confirm the reduction of the time of convergence with an increased frequency of the perturbation. The time of convergence was decreased from 6 min to 1.3 min when the delay was decreased from 30 to 5 s.

The test described previously was repeated using the MU method (Figure 7C and D) with an interval of 30 s and 5 s between external resistance changes. The change of delay did not affect the time of convergence of the MU method, which stayed around 3 min in each test. It should be noted that the optimal power output values shown in Figure 7 should not be compared with the values shown in Figures 4 and 5 since experiments related to the frequency of the perturbation were carried out one month later, and the MFC characteristics changed over time as a result of a decrease in cathode activity.

In Chioua et al,[32] it was demonstrated that excessively high-perturbation frequency in the P/O method leads to an error in optimum estimation. Results presented in Table 1 confirm this observation. This table contains the average values of external resistances to which the method converged at different time intervals between external resistance changes (resistor perturbation frequency). Clearly, if the perturbation frequency was too high, the P/O method converged to a value away from the real optimum. High-perturbation frequency when using the P/O method also introduced an overshoot in the power curve as shown in Figure 7B. The change of the time interval (i.e., delay) in the MU method did not affect the value to which the method converges. However, a very short delay resulted in variations around the optimal resistance of MFC 1. This is the effect of the instantaneous change of R at each transition from the MU adaptation period and the adaptation period.

### *Method comparison*

From analysis of the results previously presented, several conclusions can be made on the comparison of the optimization methods tested in this study. First of all, the convergence of the P/O method and the MU method were not affected by large changes in the curvature of the power curve (objective function), while the gradient method failed to optimize MFC 1. Considering the biological nature of MFCs, the change in both power output and the curvature of the power curve can be expected due to the processes of biomass growth and decay, as well as due to variations in cathode performance. Consequently, it might be difficult to achieve a stable performance using the gradient method.

The time of convergence of the MU method is shorter than the one by the P/O method. This is because the two MFCs have similar dynamics and taking the difference between them eliminates the transient effects allowing for a

**Table 1. Average Optimal Resistance Values Obtained for $\Delta R$ = 2.5 Ω and Different Time Intervals Between Resistance Changes**

| | Optimal external resistance (Ω) | | | |
|---|---|---|---|---|
| | P/O method | | MU method | |
| Time interval (s) | $R_1$ (Ω) | $R_2$ (Ω) | $R_1$ (Ω) | $R_2$ (Ω) |
| 30 | 15.2 | 19.7 | 16.6 | 17.9 |
| 10 | 13.8 | 17.1 | 16.8 | 18 |
| 5 | 12.3 | 16.1 | 17.2 | 18.4 |

faster adaptation. The same can be concluded based on the fact that the MU method is capable of accurate tracking of the optimum during a perturbation, which leads to a large and fast change in power output without changing the external resistance (electrical load). This was clearly demonstrated in the substrate test, where the optimal resistance was not changed when using the MU method. For a perturbation leading to a significant but slow change in optimal resistance, as in the temperature test, both the P/O and MU methods show excellent convergence.

The MU method showed faster convergence, but tuning of this method was more complex. *A priori* information about the differences in static characteristics is needed in order to correctly tune the MU method. In some cases, this requirement of *a priori* knowledge can be a limitation to the application of the MU method. The fast convergence of this method is subject to the similarity of the units, which are not always verified. The P/O method is simpler to tune, but the adjustment of the frequency should be done carefully to avoid a suboptimal solution or instability of the system. Excessively fast frequency of perturbation in the P/O method introduces an error of convergence on the resistance value obtained.

## Conclusion

In this article, performances of three different real-time model-free optimization methods to maximize power output delivered by two MFCs were compared. Results showed that the MU optimization method converged faster than the P/O method. Nevertheless, the performance of the P/O method was acceptable providing relatively low-perturbation frequency. The Gradient method failed to converge for one of the two MFCs tested due to large changes in the curvature of the power curve.

The P/O and MU methods were selected for performance testing during substrate and temperature variations (external perturbations). The results showed that the MU method tracks the optimum power output in the presence of an external perturbation without an unnecessary change in external resistance. The P/O method also tracked the optimum, but changes in power output caused variations in the external resistance. Overall, the P/O method can be used in a variety of MFC applications where MFC similarity is not guaranteed. On the other hand, optimal control of a stack of identical MFCs subject to fast and simultaneous changes in feed properties (i.e., presence of toxicants, pH variations, etc) can benefit from the MU optimization method.

## Acknowledgments

Assistance of Michelle-France Manuel in operating MFCs is gratefully appreciated. This work is supported by the Natural Science and Engineering Research Council of Canada (NSERC) and National Research Council of Canada (NRC publication # 50003).

## Literature Cited

1. Bond DR, Lovley DR. Electricity production by Geobacter sulfurreducens attached to electrodes. *Appl Env Microbiol*. 2005;69(3): 1548–1555.
2. Rabaey K, Boon N, Siciliano S, Verhaege M, Verstraete W. Biofuel cells select for microbial consortia that self-mediate electron transfer. *Appl Env Microbiol*. 2004;70 (9):5373–5382.
3. Reguera G, McCarthy KD, Mehta T, Nicoll JS, Tuominen MT, Lovley DR. Extracellular electron transfer via microbial nanowires. *Nature Biotechnol*. 2005;435:1098–1101.
4. Logan BE, Regan JM. Electricity-producing bacterial communities in microbial fuel cells. *Trends Microbiol*. 2006;14:512–518.
5. Liu H, Logan BE. Electricity generation using an air-cathode single chamber microbial fuel cell in the presence and absence of a proton exchange membrane. *Environ Sci Technol*. 2004;38:4040–4046.
6. Zuo Y, Cheng S, Call D, Logan BE. Tubular membrane cathodes for scalable power generation in microbial fuel cells. *Environ Sci Technol*. 2007;41:3347–3353.
7. Rabaey K, Clauwaert P, Aelterman P, Verstraete W. Tubular microbial fuel cells for efficient electricity production. *Env Sci Technol*. 2005;39:8077–8082.
8. Rabaey K, Verstraete W. Microbial fuel cells: novel biotechnology for energy generation. *Trends Biotechnol*. 2005;23 (6):291–298.
9. Tartakovsky B, Guiot SR. A comparison of air and hydrogen peroxide oxygenated microbial fuel cell reactors. *Biotechnol Prog*. 2006; 22:241–246.
10. Yu EH, Cheng S, Scott K, Logan B. Microbial fuel cell performance with non-Pt cathode catalysts. *J Power Sources*. 2007;171: 275–281.
11. He Z, Angenent LT. Application of bacterial biocathodes in microbial fuel cells. *Electroanalysis*. 2006;18(19–20):2009–2015.
12. Aelterman P, Rabaey K, Pham HT, Boon N, Verstraete W. Continuous electricity generation at high voltages and currents using stacked microbial fuel cells. *Env Sci Technol*. 2006;40:3388–3394.
13. Oh S-E, Logan BE. Voltage reversal during microbial fuel cell stack operation. *J Power Sources*. 2007;167:11–17.
14. Woodward L, Tartakovsky B, Perrier M, Srinivasan B. Maximizing power production in a stack of microbial fuel cells using multiunit optimization method. *Biotechnol Prog*. 2009;25(3):676–682.
15. Leyva R, Alonso C, I. Q, Cid-Pastor A, D. L, Martinez-Salamero L. MPPT of photovoltaic systems using extremum-seeking control. *IEEE Trans Aerosp Electron Syst*. 2006;42(1):249–258.
16. Zhong Z, Huo H, Zhu X, Cao G, Ren Y. Adaptive maximum power point tracking control of fuel cell power plants. *J Power Sources*. 2008;176:259–269.
17. Boico F, Lehman B. In: *Study of Different Implementation Approaches for a Maximum Power Tracker*. IEEE Workshop on Computers in Power Electronic, COMPEL; 2006; 15–21.
18. Wyatt J, Chua L. Power theorem, with solar application. *IEEE Trans Circuits Syst*. 1983;30:824–828.
19. Batstone DJ, Keller J, Angelidaki I, Kalyuzhnyi SV, Pavlostathis SG, Rozzi A, Sanders WTM, Siegrist H, Vavilin V. *Anaerobic digestion model no 1 (ADM1)*. London, UK: IWA Publishing; 2002.
20. Woodward L, Shadeed w, Perrier M, Srinivasan B, Suivi du point maximal de puissance de cellules photovoltaïques par la méthode d'optimisation multi-unités. In: *Conférence Internationale Francophone d'Automatique (CIFA)*, Bucarest, Romania; 2008; paper #357.
21. Boico F, Lehman B In Single sensor MPPT Algorithm for multiple solar panels configurations. PESC Record-IEEE Annual Power Electronics Specialists Conference, PESC 07-IEEE 38th Annual Power Electronics Specialists Conference; 2007; 1678–1682.
22. Xia W, Dunford G, Palmer R. Application of centered differentiation and steepest descent to maximum power point tracking. *IEEE Trans Ind Electron*. 2007;54:2539–2549.
23. Aelterman P, Versichele M, Marzorati M, Boon N, Verstraete W. Loading rate and external resistance control the electricity generation of microbial fuel cells with different three-dimensional anodes. *Bioresour Technol*. 2008;99:8895–8902.
24. Gil G-G, Chang I-S, Kim BH, Kim M, Jang J-K, Park HS, Kim HJ. Operational parameters affecting the performance of a mediator-less microbial fuel cell. *Biosens Bioelectron*. 2003;18:327–334.
25. Srinivasan B. Real-time optimization of dynamic systems using multiple units. *Int J Robust Nonlinear Control*. 2007;17:1183–1193.
26. Woodward L, Perrier M, Srinivasan B. Improved performance in the multi-unit optimization method with non identical units. *J Proc Control*. 2008;19:205–215.

27. Tartakovsky B, Manuel MF, Neburchilov V, Wang H, Guiot SR. Biocatalyzed hydrogen production in a continuous flow microbial fuel cell with a gas phase cathode. *J Power Sources*. 2008;182:291–297.
28. Hua C, Shen C. In: Comparative study of Peak Power Tracking Techniques for Solar Storage Systems. IEEE Applied Power Electronics Conference and Exposition, Anaheim, CA; 1998; 679–683.
29. Nocedal J, Wright SJ. *Numerical Optimization*. New York: Springer; 2006.
30. Logan BE, Call D, Cheng S, Hamelers HVM, Sleutels THJA, Jeremiasse AW, Rozendal RA. Microbial electrolysis cells for high yield hydrogen gas production from organic matter. *Env Sci Technol*. 2008;42:8630–8640.
31. Siegrist H, Vogt D, Garcia-Heras JL, Gujer W. Mathematical model for meso- and thermophilic anaerobic sewage sludge digestion. *Env Sci Technol*. 2002;36:1113–1123.
32. Chioua M, Srinivasan B, Guay M, Perrier M. Dependence of the error in the optimal solution of perturbation-based extremum seeking methods on the excitation frequency. *Can J Chem Eng*. 2007;85(4):447–453.

*Manuscript received Jun. 19, 2009, and revision received Nov. 6, 2009.*